POLITECNICO DI TORINO
Repository ISTITUZIONALE

MultiphysicsEnabled Liquid State Thermal Harvesting: Synergistic Effects between Pyroelectricity and Triboelectrification

Original
MultiphysicsEnabled Liquid State Thermal Harvesting: Synergistic Effects between Pyroelectricity and Triboelectrification / Chiolerio, A., Garofalo, E., Bevione, M., Cecchini, L.. - In: ENERGY TECHNOLOGY. - ISSN 2194-4288. - (2021), p. 2100544. [10.1002/ente.202100544]

Availability:
This version is available at: 11583/2922533 since: 2021-09-09T11:58:05Z

Publisher:
John Uhlrich

Published
DOI:10.1002/ente.202100544

Terms of use:

This article is made available under terms and conditions as specified in the corresponding bibliographic description in the repository

Publisher copyright

(Article begins on next page)

19 November 2026

Check for updates

Energy Technology
Generation, Conversion, Storage, Distribution
www.entechnol.de

Multiphysics-Enabled Liquid State Thermal Harvesting: Synergistic Effects between Pyroelectricity and Triboelectrification

Alessandro Chiolerio, Erik Garofalo, Matteo Bevione, and Luca Cecchini*

Energy consumption levels show a never-ending increase since the industrial era. Toward sustainability objectives, it is of outstanding importance to reduce the amount of wasted energy, that typically comes as waste heat, as a consequence of nonunitary efficiency of any thermodynamic process. Herein, a breakthrough in conversion of low enthalpy heat into electricity is presented, based on a liquid state device that operates through multiphysics effects: thermomagnetic advection, triboelectricity, pyroelectricity, and Ludwig–Sorét effect. A synergistic interaction between ferroelectric surfaces and a complex composition colloidal suspension is evidenced, owing to an enhancement of the generated potential of 365% in comparison with pyroelectric effect and 267% in comparison with triboelectric effect, while the current extracted is 54% higher than the pyroelectric effect only and the power extracted by induction remains substantially unperturbed. The impact of this technology on society is also analyzed, on the basis of a set of practical applications, by means of a computational analysis.

1. Introduction

A recent study reveals that world energy consumption has been monotonically rising since the second half of 1800s, and is expected to achieve in 2040 more than 200 000 TWh year^{-1}.[1] In view of this, energy-related issues including location and exploitation of resources, extraction and shipment costs, transformation and distribution, accessibility and dynamic demand, as well as awareness about utilization, should be carefully pondered, in the sustainable development of our society. Considering that 72% of energy consumption is wasted in form of heat, it is easy to understand how waste heat recovery (WHR) technologies can generate wealth in a sustainable way, meanwhile reducing the environmental impact of technological activities.[2] In particular, waste heat to power (WHP) represents the process of converting the heat discarded by an existing process and using that same heat to generate electricity, mainly due to thermodynamic cycles and solid state devices, such as thermoelectric ones.[3] Thermoelectric devices partially solve those problems but suffer the drawbacks of using expensive and eventually toxic materials, reaching optimal performances in often narrow temperature ranges.

A novel and sustainable approach to harvest and convert into power waste heat is based on the employment of liquid state functional colloids, suspensions of nanoparticles (NPs) dispersed in a carrier solvent whose dynamics is activated by Rayleigh–Bénard-like convection movements: the higher the gradient, the faster is the convection dynamics. Such approach has been called Colloidal EneRgEtic System (CERES),[4] and it can be designed to recover energy in different operational environments, making use of synergistic physical effects. In particular, electromagnetic induction can be exploited whenever the highest working temperature is below the Curie temperature of the magnetic component of the system, meaning that the materials choice is the real limiting feature.[5] Triboelectricity can be exploited collecting the displaced charges generated by fluid motion and friction with the inner walls of a pipeline, especially in situations with a small thermal gradient to exploit.[6] On the contrary, pyroelectricity can be exploited more profitably in those situations where the available thermal gradient is as high as hundreds of K.[7] CERES systems have been shown to harvest temperature gradients as small as 1 K, in a range comparable with microbial fuel cells of tens of μW K^{-1}, with an efficiency approaching 20% of Carnot efficiency of an ideal thermal machine working on the same temperature difference.

In this work, we have explored to what extent a multieffect conversion system can be exploited by combining together the effects

A. Chiolerio,[+] E. Garofalo, M. Bevione,[++] L. Cecchini[+]
Center for Sustainable Future Technologies
Istituto Italiano di Tecnologia
10144 Torino, Italy
E-mail: alessandro.chiolerio@iit.it

E. Garofalo
Electronics and Telecommunications Department
Politecnico di Torino
10120 Torino, Italy

The ORCID identification number(s) for the author(s) of this article can be found under https://doi.org/10.1002/ente.202100544.

[+]Present address: Bioinspired Soft Robotics Laboratory, Istituto Italiano di Tecnologia, 16163 Genova, Italy

[++]Present address: Laboratory for High Performance Ceramics, EMPA Swiss Federal Laboratories for Materials Science and Technology, 8600 Dübendorf, Switzerland

© 2021 The Authors. Energy Technology published by Wiley-VCH GmbH. This is an open access article under the terms of the Creative Commons Attribution License, which permits use, distribution and reproduction in any medium, provided the original work is properly cited.

DOI: 10.1002/ente.202100544

of thermomagnetic advection, triboelectricity, and pyroelectricity, using a mixed colloid and focusing on synergistic effects that could arise and make such technology particularly profitable.[8]

2. Results and Discussion

2.1. System Overview

The test bed is a linear apparatus (**Figure 1**a), where a peristaltic pump is used to control the colloid velocity, mimicking the effects of Rayleigh–Bénard,[9] or magneto-Rayleigh–Bénard convection and letting us to associate with local velocity changes in the ideal energy recovery.[10,11] To do that, the colloid is stored in a becher where a magnetic stirrer maintains its compositional and thermal homogeneity, while a heating plate provides the desired thermal power (Figure 1a). Then it is pumped inside a fluorinated ethylene propylene (FEP) pipe, a particular material whose molecular structure is suitable to guarantee a proper triboelectrification via surface shear, compatibly with the nanoparticles of choice.[6] Three extraction systems are installed: 1) a titanium-resistive electrode, placed directly in contact with the colloid collecting charges by mechanical drag; 2) an oxygen-free copper (OFC) solenoid wound around the pipe, collecting charges by induction; and 3) an aluminum capacitive electrode placed externally, in contact with the pipe, collecting charges by dielectric polarization. Each electrode can be coupled with one of the functional components of the colloid, showing pyroelectric, magnetic, and triboelectric properties, respectively: 1) barium titanate (BT) 300 nm nanoparticles (NPs); 2) a ferrofluid (FF) based on magnetite 10 nm NPs capped with oleic acid; and 3) titania (T) 50 nm NPs. While it is clear that BT and T NPs, having no net magnetization, can provide no induction, we will see how the pure triboelectric component is greatly enhanced by the mixed colloid, as well as the pyroelectric component, by synergistic effects. The inductive component remains unperturbed.

The FEP pipe itself features a ferroelectric behavior (Figure 1b); therefore, it is possible to bring the polymer to an electrical remanence state and take advantage of its dielectric displacement in the shear interaction with the moving colloid and NP surfaces. The polarized pipe rotates the polarization of incoming NPs on the fluid boundary layer; their surface charge is being generated due to mechanical friction (triboelectricity), to temperature temporal gradients (pyroelectricity), or to temperature spatial gradients (Ludwig–Sorét effect).[12] We can think at the system as a spring: the spring stores energy until the pipe is brought to its electrical remanence state, where it can polarize the charges of the moving fluid and increase conversion efficiency. When the colloid moves very fast along a specific direction (say forward), the friction between the fluid and the pipe walls can rotate the pipe polarization state and eventually reach its electrical coercivity, where the net polarization is zero (the spring is released). Here, the pipe is not anymore able to polarize the fluid and we lose conversion efficiency. If the same forward direction is preserved, the fluid can transfer again energy on the pipe walls and bring their polarization to the negative remanence, restoring its polarization capabilities and conversion efficiency (by analogy the spring is again compressed). Apart from the mechanical analogy with a spring, an electrical analogy holds true: the resistive titanium electrode permits to harvest charge accumulated in the fluid whose equivalent is a voltage generator, while the colloid itself acts as a primary circuit. This circuital analogue holds even when the external velocity of the fluid is zero: spatial temperature gradients are able to initiate density gradients by diffusion, which ultimately produce an electromotive force on the inner electrode (see Supporting Information).

2.2. Resistive Electrode

In the experiment we decided to decouple velocity and temperature gradients, controlling both of them, in view of practical applications, where harvesting devices can be thought of taking advantage of other sources of kinetic energy, such as the gravitational potential. When the fluid is set in motion, charge carriers are transferred by direct contact with the resistive electrode and measured, showing typical short-circuit current profiles as in **Figure 2**a, in the range of tens of nA. The potential that settles on the resistive electrode can be in the range of hundreds of V, with speeds ranging between 0.22 mm s^{-1} and 2.2 cm s^{-1}, as shown in Figure 2b (speeds have been labeled to each corresponding peak). Interesting is to notice that it is sensitive

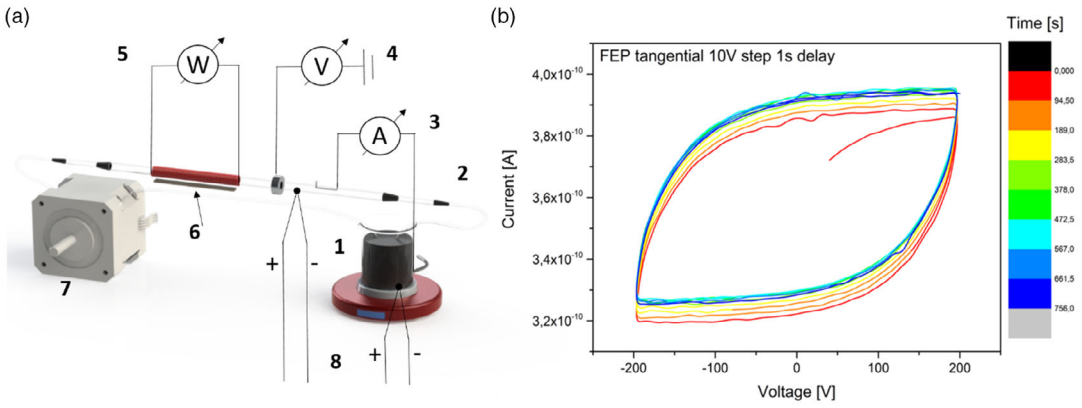


Figure 1. a) 3D rendering of the multiphysics CERES: 1—becher with colloid reservoir, 2—FEP pipe, 3—resistive electrode with ammeter, 4—capacitive electrode with voltmeter, 5—inductive electrode with power meter, 6—permanent magnets stack, 7—peristaltic pump, and 8—thermocouples for gradient monitoring. b) Electrical minor hysteresis loop recorded along the tangential direction of a FEP pipe.

© 2021 The Authors. Energy Technology published by Wiley-VCH GmbH

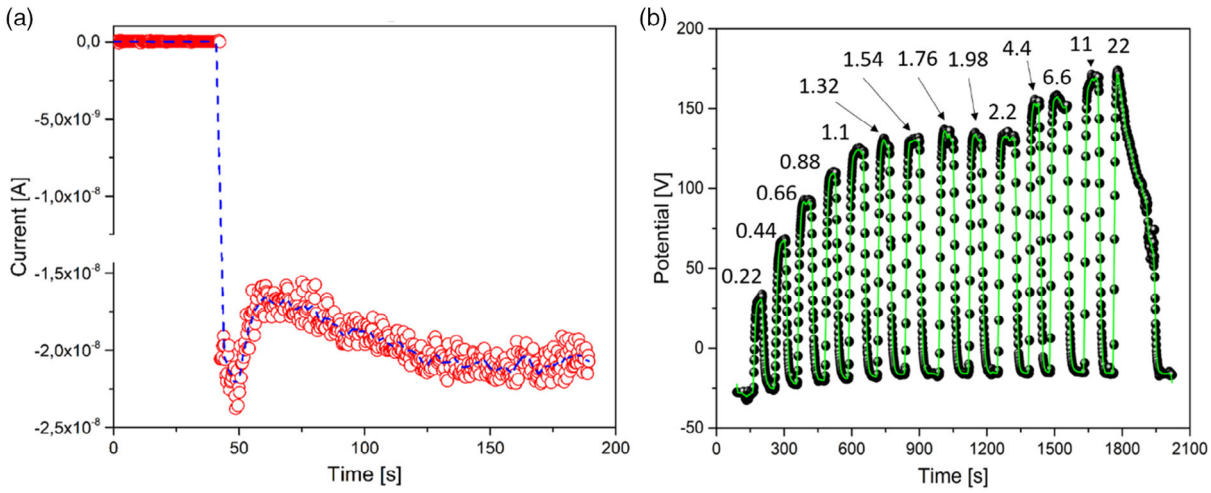


Figure 2. a) Typical profile of current extracted exploiting the resistive electrode, system heated at 60 °C, and mixed colloid pumped at a speed of 2.2 cm s^{-1}. b) Typical profile of potential measured on the resistive electrode, system undergone impulses at increasing speeds, ranging from 0.22 mm s^{-1} to 2.2 cm s^{-1}, at room temperature. The number close to each potential peak indicates the corresponding speed in mm s^{-1}.

to the magnitude and direction of the colloid velocity: inverting the flux an inversion of the potential sign is observed (here the pipe polarizes in the opposite direction and operates therefore its effect on the fluid as per the spring analogy), similar to what happens with electrochemical batteries. By comparing the multiphysics setup with mixed composition colloid with an experiment conceived to evaluate only the pyroelectric effect where the colloid was limited to FF and BT components, we can state that the generated potential is approximately 365% higher and the current is 54% higher.[7] This remarkable result is a first proof of the synergistic effects enabled in the current setup. Owing to natural dispersions in the liquid circuit, the system thermalizes with relaxation times in the order of 1 h. The Maxwell heating effect provided by magnetic stirring can be easily measured (see Supporting Information) as a 1.1 K temperature difference between the becher and the full pipe.

2.3. Inductive Electrode

The inductive electrode extraction relies upon the magnetic flux change due to magnetic momenta carried by flowing FF, whose effect on the coil is that of inducing a small electromotive force and a current consistent with power up to the hundreds of pW range, as shown in **Figure 3**a. By comparing the multiphysics experiment with a similar one conceived to exploit thermomagnetic advection, we have for the former an optimal thermal conversion of 3.25 nW K^{-1} (see Supporting Information) while for the latter 10.4 μW K^{-1}; considering that the concatenated magnetic flux is directly proportional to the coil area times the number of windings squared, and given the built geometrical parameters of the two setups, we have a ratio 1:2750 meaning that the current setup could be able to provide 9 μW K^{-1} under similar built geometries.[5] The induction electrode has an extremely low resistance of 421 ± 1 mΩ (see Supporting Information), which is a preferred feature necessary not to waste the generated potential in internal resistance. Of course, this inductive effect is not influenced by the other components of the colloid that do not possess magnetic momentum but is subject to temperature effects in reason of the Curie–Weiss law and temperature dependence of magnetic anisotropy, ultimately influencing the collective behavior of the colloid.[13] A complete analytical model has been developed to independently take into account the effects of magnetic field (provided by the permanent magnets stack), temperature, and concentration of FF.[14]

2.4. Capacitive Electrode

The external capacitive electrode provides an additional source of electrostatic energy due to a coupling with the FEP pipe, the displacement of charges by means of the moving colloid and the mechanical transfer to the dielectric pipe walls charges the cylindrical capacitor and stores energy, in a way similar to a Van de Graaf generator (see Figure 3b). By comparing the multiphysics setup potential accumulated on the capacitive electrode (see Supporting Information) with a setup conceived to exploit triboelectricity with a colloid based on T only, we can see at room temperature that the maximum potential extracted is 267% higher. Furthermore, the current setup allows an optimal extraction when a working thermal gradient is submitted to the colloid, achieving in this case a top performance of 1000% higher than the corresponding triboelectric converter at room temperature.

2.5. Maximum Power Analysis and Depolarization Effect

The velocity profiles as a function of acquisition time (**Figure 4**a,b) show the fast dynamics of the system in collecting harvested energy even at speeds <1 mm s^{-1}: data are shown in open- and closed-circuit configurations using the resistive electrode. Typical Rayleigh–Bénard convection, with a thermal gradient of 1 K, is known to generate diffusive patterns as fast as 1.19 cm s^{-1}.[15] Our system, using the three collection means simultaneously, provides a maximum power output of 700 nW at 1 cm from the three collection means a maximum power output of

© 2021 The Authors. Energy Technology published by Wiley-VCH GmbH

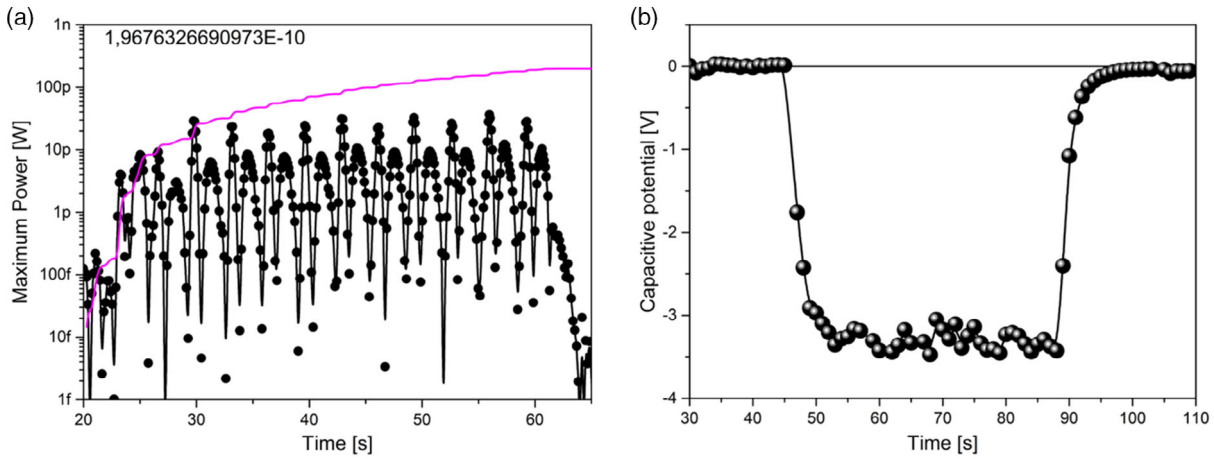


Figure 3. a) Power output of the inductive electrode at 65 K when the colloid is pumped at 0.22 mm s^{-1}. b) Typical potential recorded on the capacitive electrode in an experiment run in strong heating (35 K temperature gradient) and with pumping at a speed of 6 mm s^{-1}.

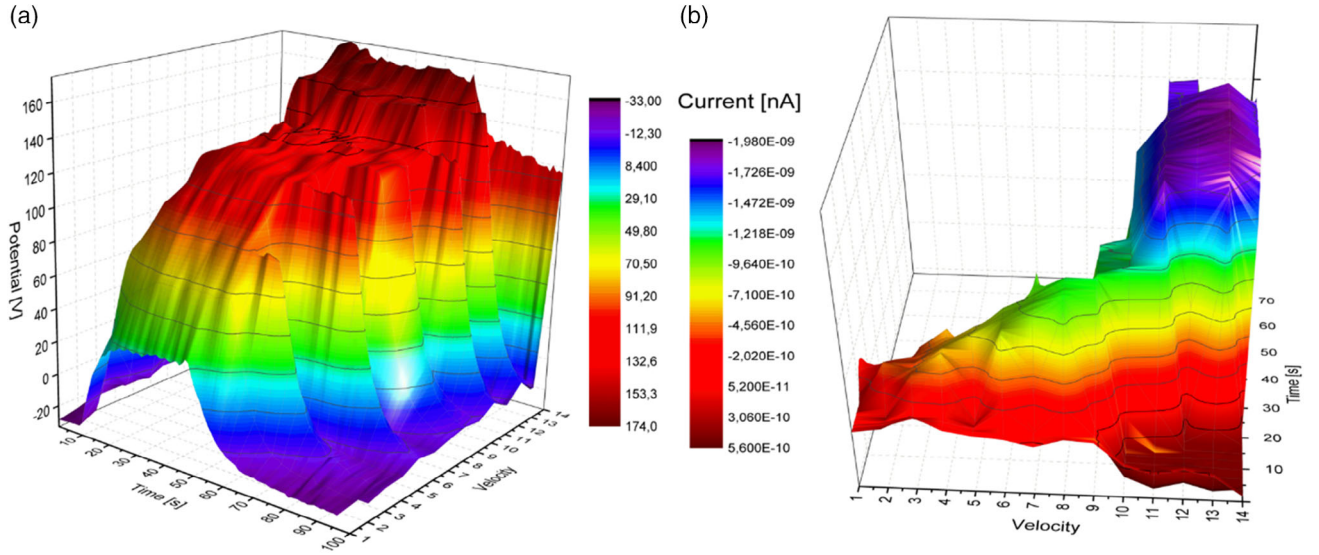


Figure 4. a) Potential surface as a function of acquisition time and colloid velocity in open circuit condition, collected by the resistive electrode at room temperature. b) Current surface as a function of acquisition time and colloid velocity in closed circuit condition, collected by the resistive electrode at room temperature.

700 nW, while 150 nW is available at 1 mm s^{-1}, equivalent to a thermal gradient of 0.1 K. In the former case we reached an equivalent efficiency of 38% with respect to the ideal Carnot cycle of a thermal machine working across the same temperature gradient, while in the latter case the efficiency reaches 60% of the ideal Carnot. This result tells us that achieving lower efficiencies with higher speeds can be justified with the increased effects of dynamical viscosity. As said, the liquid circuit behaves also as an electrodynamic brake: the continuous friction of NPs on the FEP pipe moves the working point along the ferroelectric hysteresis cycle and reduces the remanent polarization, as we can learn from the analysis of voltage peaks from Figure 2b, as shown in **Figure 5**a. We fitted each plateau with a linear function and plotted their intercept, slope, and *R* square factor as a function of speed, for the room-temperature and a high-temperature gradient cases. It can be seen that the slope remains close to zero (perfectly horizontal plateau of voltage reached at each speed) until speeds of 1 cm s^{-1}, turning to negative for higher speeds (the plateau now becomes a steep curve where the voltage collected decreases, losing in conversion efficiency). This phenomenon is perfectly exponential with respect to velocity and can be avoided by operating the converter in a safe region to avoid depolarization. The power specific to colloid volume is shown in Figure 5b, based on room temperature measurements taken from the resistive electrode. Here, the pure potential was converted to electric field considering the distance between resistive electrode and reference electrode in the becher; the pure current was converted to current density considering the electrode

© 2021 The Authors. Energy Technology published by Wiley-VCH GmbH

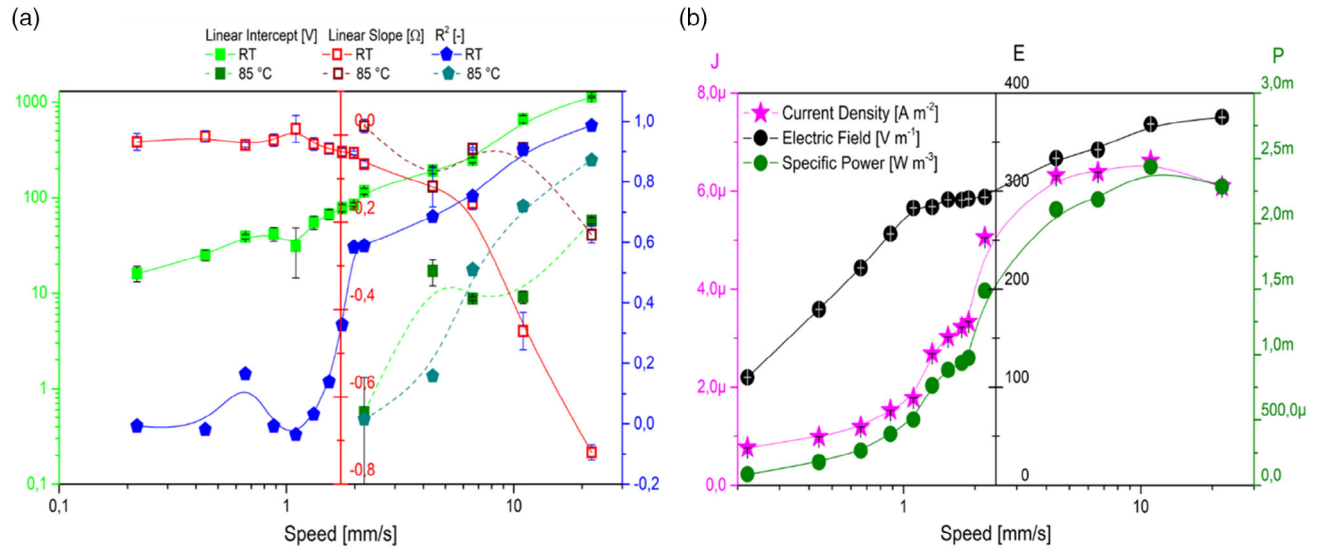


Figure 5. a) Linearity factors (intercept and slope) and related errors extracted from linear fits to potential plateaus shown in Figure 2b, highlighting the depolarization of FEP pipe walls by triboelectric interaction with moving colloid, occurring at higher velocities. b) Effect of speed on electric field, current density, and overall specific power measured on the resistive electrode at room temperature.

surface; and the maximum power as product of the potential times current was converted to a volume-specific quantity considering the mixed colloid volume. The maximum power output is achieved at a pumping speed of 1 cm s^{-1}, roughly corresponding to a thermal gradient of 1 K.

Recorded currents from the inductive electrode are extracted as the average value over measurements as a function of colloid speed, even though both current and voltage coupled with the liquid FF circuit feature both a positive and a negative spike, consistent with the fluid entering (exiting) the coil region and inducing a positive (negative) electromotive force. Nevertheless, the average is always nonzero, due to the natural asymmetries present in the system, most importantly the magnetic field provided by permanent magnets used to magnetize the fluid and break the symmetry of the setup, and features quite a big standard deviation. A maximum power output of 3.3 nW is achieved just above 1 mm s^{-1} of speed (**Figure 6**a), while a plateau around 500 pW can be found for speeds above 2 mm s^{-1}, indicating that viscous phenomena, such as the formation of a slow boundary layer and a faster core in the pipe section, can reduce the efficiency of magnetoinductive power conversion. For what concerns the capacitive potential, an optimal working point can be found at 1 mm s^{-1}, where the pipe walls can operate at their ferroelectric remanence. Increasing the speed enhances walls depolarization down to electric coercivity, where the measured potential is zero (4 mm s^{-1}); a further

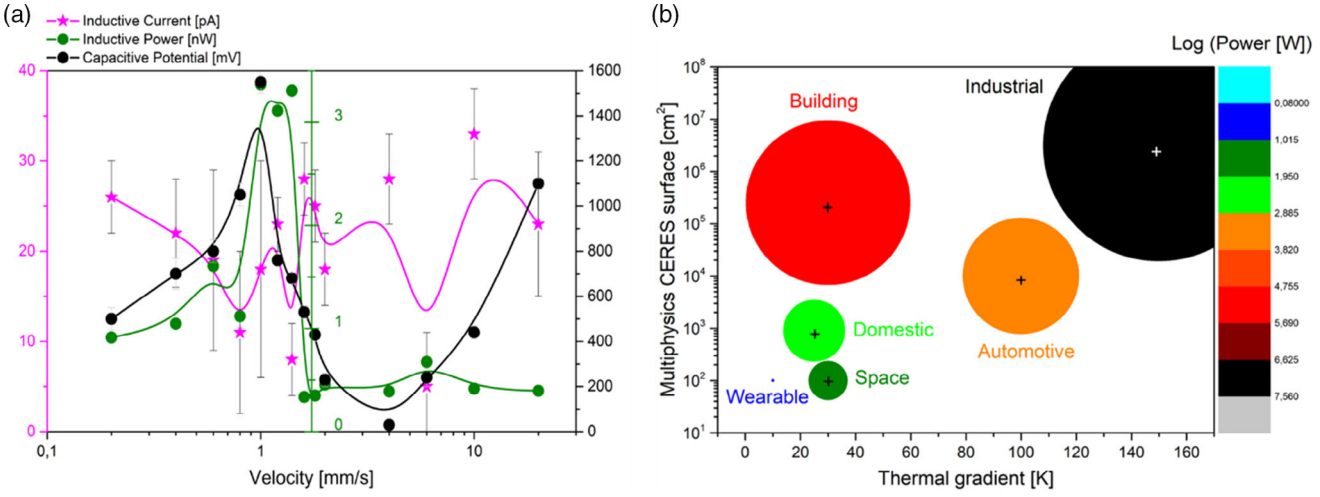


Figure 6. a) Effect of speed on inductive current and overall power as well as capacitive potential, measured at room temperature. b) Application scenarios of the multiphysics CERES converter as per numerical analysis. The bubble diameter and color are proportional to log (power), each use case is defined by the working thermal gradient and the exchange surface with a hot/cold reservoir.

© 2021 The Authors. Energy Technology published by Wiley-VCH GmbH

Table 1. Parameters used to perform numerical analysis of the energy conversion impact given by the liquid state multiphysics thermal harvesting.

Application	Device thickness [m]	Device area [m^2]	Working thermal gradient [K]	Conversion power [W]
Wearable	0.05	0.01	10	395 μ
Space	0.1	0.01	30	6 m
Domestic	0.15	0.1	25	33 m
Automotive	0.2	1	100	2
Building	0.07	25	30	73
Industrial	0.5	1500	150	11 k

increase in speed restores the polarization effect of the walls and the measured capacitive potential.

2.6. Numerical Scale-Up Analysis

In order to estimate the impact on society of a multiphysics CERES WHP system, typical application scenarios have been hypothesized and summarized in **Table 1**, in particular defining practical application domains and reasonable device geometries in terms of thickness and surface are. Foreseen domains are: a wearable patch, a conversion device for space satellites and launchers, an add-on for domestic appliances that generate waste heat such as refrigerators and ovens, an add-on for automotive applications to be coupled with the heat exchanger of the engine, a panel to install in a building wall to reduce wasted heat from inside/incoming radiation from outside, and a standard industrial application. Through a script we computed the power produced in a conversion apparatus exploiting the same features reported in our experiments: colloidal mixture components and volumetric concentration, but different geometry and therefore volume of colloid exploited. Outcomes can be visualized both in the last column of Table 1 and in Figure 6b. The complete script is reported in Supporting Information. Continuously extracted power ranges from 395 μW of the wearable device to 11 kW of an industrial apparatus operating over 150 K of gradient. No materials optimization was considered in such analysis, while it is clear that progress in utilizing higher efficiency colloid mixtures could easily increase the amount of energy extracted.

3. Conclusions

The technology we have so far described is potentially able to recover quite a wide amount of energy currently wasted into the environment, in a specific field, that of low enthalpy reservoirs, where little if any at all solutions are available. We have described a conversion device based on a liquid state suspension that operates through multiphysics effects: thermomagnetic induction, triboelectricity, pyroelectricity, and Ludwig–Soret effect. A synergistic interaction between ferroelectric surfaces and a complex composition colloidal suspension is evidenced, owing to an enhancement of the generated potential of 365% in comparison with pyroelectric effect and 267% in comparison with triboelectric effect, while the current extracted is 54% higher than the pyroelectric effect only and the power extracted by induction remains substantially unperturbed. Before a real application can be met, some further efforts in colloid synthesis and stabilization are needed, so that the NPs do not settle and are kept at distance, thus avoiding aggregation. We believe that, owing to the huge literature in colloids, stable multifunctional colloids appear easy to achieve. Operation at higher temperatures should also be improved: as FF is based on a hydrocarbon solvent, tubings made in polyamide can swell and lose in tightness. This swelling is enhanced at higher temperatures, making it almost impossible to run liquids at temperatures higher than 95 °C. Nevertheless, a clever choice of materials and components for the colloid should allow operational temperatures as high as the solvent boiling point, therefore up to the range of 200–250 °C. To allow operation at temperatures higher than 300 °C, one should move to inorganic solvents, ionic liquids, or alike.[16]

Industrial low enthalpy (<150 K ΔT) recoverable energy amounts to 14 000 TWh $year^{-1}$ and based on our efficiency estimates, the multiphysics CERES could allow to recover up to 2900 TWh (approximately worth 290 €B $year^{-1}$) and avoid the emission of 986 MTonn of CO_2.

4. Experimental Section

Kerosene (purchased from Carlo Erba) was chosen as solvent because of its compatibility with the FF carrier, FF was mixed in reason of 2 vol% (Ferrotech EFH3), BT NPs (purchased from Inframat Advanced Materials) added in quantity equal to 1 vol% of the overall mixture, and T NPs (Evonik Degussa, Essen, Germany) also added to 1 vol%. The particles were dispersed by ultrasonication using a horn sonicator (Branson Digital Sonifier Model 450) performed for 30 min at 100 W, with a duty cycle of 10 s of rest each 10 s of operation. To ensure homogeneous dispersion during the entire duration of the experiments, a magnetic stirrer (Velp Scientifica) was used. This is equipped with a heating plate used to heat the suspension. The peristaltic pump (Ismatec MCP) is equipped with a rotor system coupled with silicone pipes having outer diameter (OD) of 4 mm and inner diameter (ID) of 3.2 mm. The central part of the apparatus is a FEP pipe having OD = 12 mm and a larger ID = 10 mm, and hosts a resistive titanium electrode (purchased from Sigma-Aldrich, purity 99.98%) having a width of 5 mm, length of 30 mm, and thickness of 0.2 mm, a capacitive aluminum electrode in the form of a screw clamp having an ID of 12 mm an OD of 28 mm and a length of 9 mm, and an inductive electrode made by coiling a copper wire around the FEP pipe (30 turns, single layer). To create the hydraulic connection, two further pipes (having OD = 7 mm and OD = 10 mm) have been used, connecting them with some tube glass reinforced nylon 6.6 connectors (purchased by Legris, series LF 3000). Temperature was monitored by means of N-type thermocouples (Eltec Cables and Instruments), calibrated and connected to a Data AcQuisition (DAQ) system (USB-6289 by National Instrument) controlled by means of LabView program for data manipulation. The resistive electrode is sealed using high-strength two-component epoxy adhesive LOCTITE EA 9455 (purchased from Henkel). Voltage and current versus time on both resistive and capacitive electrodes are acquired by means of two identical Keithley 2635A–SourceMeter controlled remotely by LabView program for the data acquisition. Voltage and current on the inductive electrodes have been measured using a Keithley 4200-SCS Semiconductor Characterization System coupled with a Keithley 4225-RPM Remote Amplifier (Tektronix, Inc., Beaverton, OR, USA).

© 2021 The Authors. Energy Technology published by Wiley-VCH GmbH

Supporting Information

Supporting Information is available from the Wiley Online Library or from the author.

Acknowledgements

Open Access Funding provided by Istituto Italiano di Tecnologia within the CRUI-CARE Agreement.

Conflict of Interest

The authors declare no conflict of interest.

Author Contributions

A.C. contributed to supervision, funding, methods, experiments, data analysis, and draft writing, editing; E.G. contributed to methods, experiments, data analysis, graphics, and editing; M.B. contributed to methods, experiments, data analysis, numerical simulations, and editing; and L.C. contributed to methods, experiments, data analysis, and editing.

Data Availability Statement

Research data are not shared.

Keywords

barium titanate, magnetite, pyroelectricity, titania, triboelectricity, waste heat to power

Received: June 22, 2021
Revised: August 7, 2021
Published online:

[1] V. Smil, *Energy Transitions-History, Requirements, Prospects*, 1st ed., ABCCLIO, Santa Barbara, CA **2010**.
[2] C. Forman, I. K. Muritala, R. Pardemann, B. Meyer, *Renew. Sustain. Energy Rev.* **2016**, *57*, 1568.
[3] E. Garofalo, M. Bevione, L. Cecchini, F. Mattiussi, A. Chiolerio, *Energy Technol.* **2020**, *8*, 2000413.
[4] A. Chiolerio, M. B. Quadrelli, *Energy Technol.* **2019**, *7*, 1800580.
[5] A. Chiolerio, E. Garofalo, F. Mattiussi, M. Crepaldi, G. Fortunato, M. Iovieno, *Appl. Energy* **2020**, *277*, 115591.
[6] E. Garofalo, L. Cecchini, M. Bevione, A. Chiolerio, *Nanomaterials* **2020**, *10*, 1181.
[7] M. Bevione, E. Garofalo, L. Cecchini, A. Chiolerio, *MRS Energy Sustain.* **2020**, *7*, 38.
[8] S. A. Suslov, A. A. Bozhko, A. S. Sidorov, G. F. Putin, *Phys. Rev. E* **2012**, *86*, 16301.
[9] P. Berge, M. Dubois, *Contemp. Phys.* **1984**, *25*, 535.
[10] T. Yanagisawa, Y. Hamano, T. Miyagoshi, Y. Yamagishi, Y. Tasaka, Y. Takeda, *Phys. Rev. E* **2013**, *88*, 063020.
[11] T. Zürner, F. Schindler, T. Vogt, S. Eckert, J. Schumacher, *J. Fluid Mech.* **2020**, *894*, A21.
[12] W. Köhler, K. I. Morozov, *J. Non-Equilib. Thermodyn.* **2016**, *41*, 151.
[13] Y. Dikansky, A. Ispiryan, S. Kunikin, N. Perov, A. Semisalova, *EPJ Web Conf.* **2018**, *185*, 09011.
[14] L. Cecchini, A. Chiolerio, *J. Phys. D: Appl. Phys.* **2021**, *54*, 355002.
[15] W. Kays, M. Crawford, B. Weigand, *Convective Heat and Mass Transfer*, 4th ed., McGraw-Hill Professional, New York **2004**.
[16] A. Chiolerio, M. B. Quadrelli, *Adv. Sci.* **2017**, *4*, 1700036.

© 2021 The Authors. Energy Technology published by Wiley-VCH GmbH